Clim. Past Discuss., 10, 3421–3447, 2014
www.clim-past-discuss.net/10/3421/2014/
doi:10.5194/cpd-10-3421-2014

Climate of the Past Discussions
Open Access

Using beryllium-10 to test the validity of past accumulation rate reconstruction from water isotope records in East Antarctic ice cores

A. Cauquoin[1], A. Landais[1], G. M. Raisbeck[2], J. Jouzel[1], L. Bazin[1], M. Kageyama[1], J.-Y. Peterschmitt[1], M. Werner[3], E. Bard[4], and ASTER Team[4,*]

[1]Laboratoire des Sciences du Climat et de l'Environnement (LSCE/IPSL, CEA-CNRS-UVSQ), CEA Saclay Orme des Merisiers, 91191 Gif-sur-Yvette, France
[2]Centre de Sciences Nucléaires et de Sciences de la Matière (CSNSM), UMR CNRS 8609, Université Paris Sud XI, Bât 108, 91405 Orsay, France
[3]Alfred Wegener Institute for Polar and Marine Research (AWI) Bussestraße 24, 27570 Bremerhaven, Germany
[4]Aix-Marseille Université, CNRS-IRD-Collège de France, UM 34 CEREGE, Technopôle de l'Environnement Arbois-Méditerranée, BP80, 13545 Aix-en-Provence, France
[*]M. Arnold, G. Aumaître, D. L. Bourlès and K. Keddadouche

Received: 18 July 2014 – Accepted: 1 August 2014 – Published: 22 August 2014

Correspondence to: A. Cauquoin (alexandre.cauquoin@lmd.jussieu.fr)

Published by Copernicus Publications on behalf of the European Geosciences Union.

CPD

10, 3421–3447, 2014

Abstract

Ice cores are exceptional archives which allow us to reconstruct a wealth of climatic parameters as well as past atmospheric composition over the last 800 ka in Antarctica. Inferring the variations of past accumulation rate in polar regions is essential both for documenting past climate and for ice core chronology. On the East Antarctic plateau, the accumulation rate is so small that annual layers cannot be identified and accumulation rate is mainly deduced from the water isotopic composition assuming constant temporal relationships between temperature, water isotopic composition and accumulation rate. Such assumption leads to large uncertainties on the reconstructed past accumulation rate. Here, we use high resolution beryllium-10 (^{10}Be) as an alternative tool for inferring past accumulation rate for the EPICA Dome C ice core, in East Antarctica. We present a high resolution ^{10}Be record covering a full climatic cycle over the period 269 to 355 kyr BP from MIS 9 to MIS 10 (Marine Isotope Stages). After correcting ^{10}Be for the estimated effect of the paleomagnetic field, we deduce that the classical estimation of accumulation rate variations from records of water isotopes agrees, with a possible underestimation of 16 %, with the uncertainty on the temperature reconstruction from water isotopes in Antarctic ice cores. This is within their uncertainty of −10 to +30 %. Finally, we show that the relationship between temperature and accumulation rate is comparable when using ice core data and results from several AGCM simulations run on glacial–interglacial conditions despite a larger spread in model outputs. These results indicate that the thermodynamic law linking moisture content in the air and temperature, as implemented in the different models, leads to realistic results even in polar regions, at the end of the water distillation trajectory.

1 Introduction

Polar ice cores provide reference records for past climatic conditions over the last 130 ka (thousands of years) in Greenland (North Greenland Ice Core Project Members, 2004; NEEM Community Members, 2013) and over the last 800 ka in Antarctica (EPICA Community Members, 2004). That ice as old as 800 kyr BP (kiloyears Before Present) can be retrieved at a depth of 3200 m is due to the very low accumulation rate encountered at this site of the East Antarctic Plateau (2.73 cm ice equivalent per year today, EPICA Community Members, 2004). Accumulation rate is even smaller during glacial periods as expected from simple thermo-dynamical considerations: cold air holds less moisture than warm air. Still, the quantitative reconstruction of past accumulation rate is not straightforward and large uncertainties (> 30 %) are often associated with its reconstruction in polar ice cores (Blunier et al., 2007; Guillevic et al., 2013; van Ommen and Morgan, 1997).

Reducing the uncertainties on the reconstruction of past accumulation rate is essential for several reasons. First and most obviously, this will lead to an improved ice core chronology. Second, even if the physical relationship between air moisture content and temperature holds true with time, there is no a priori reason why the link between accumulation rate and temperature should be constant with time in polar regions, at the very end of the water distillation process. Some decoupling can be expected between accumulation rate and temperature or water isotopes from which polar temperature is classically retrieved. Finally, reducing the uncertainties in the accumulation rate reconstruction and in the link between accumulation rate and temperature in polar region is a stringent test for climate models. There is thus a clear need for temperature – and water isotope – independent estimates of past accumulation changes.

In this study, we recall the classical way to deduce the accumulation rate in polar ice cores from water isotope measurements. In order to obtain independent estimates, we confront it to outputs of General Circulation Model simulations for the Last Glacial Maximum (LGM) and the present day. Thirdly, we explore the use of beryllium-10 (^{10}Be), a cosmogenic isotope to obtain an independent estimate of past accumulation. After their production in the upper atmosphere (Lal and Peters, 1967), ^{10}Be atoms become fixed to aerosols and fall very quickly (within 1–2 years according to Raisbeck et al., 1981a) on the Antarctic plateau primarily by dry deposition. A simplistic assumption namely that the ^{10}Be flux is constant through time has been applied to estimate accumulation changes along the Vostok ice core, first from a limited set of measurements (Yiou et al., 1985) and then from a more detailed, but still low resolution and discontinuous data set covering the last climatic cycle (Jouzel et al., 1989). However, the assumption of a constant ^{10}Be flux is limited by the heliomagnetic and geomagnetic modulations: the higher these fields are, the more primary cosmic ray particles are deflected which leads to a decrease of cosmogenic isotope production. For example, this problem is important for the last glacial period which includes the Laschamp excursion, a dramatic short-lived decrease in the Earth's magnetic field intensity occurring about 41 kyr ago (Singer et al., 2009).

In the present study, we exploit a continuous and very detailed ^{10}Be time series covering a full climatic cycle over a 86 ka-period, from MIS 9 to MIS 10 (Marine Isotope Stages), measured along the Dome C ice core (75°06′ S, 123°21′ E). Two geomagnetic events are mentioned during this time range at 290 kyr BP (so-called "Portuguese Margin" Thouveny et al., 2008) and 320 kyr BP (so-called "Calabrian Ridge 1" Langereis et al., 1997).

Our manuscript is organized as follows. After a reminder of the classical estimation of past accumulation rates from water isotopes in ice core and a presentation of the procedure, we examine the multidecadal ^{10}Be record and discuss how this ∼ 86 ka long record allows inferring information about the associated glacial–interglacial accumulation rate change. In the following section, we discuss the relationship between temperature/δD and accumulation rate changes on the East Antarctic plateau over deglaciations using constraints both from glaciological data and from a bunch of modeling outputs inferred from 11 different Coupled Ocean–Atmosphere General Circulation Models (AOGCMs) and 1 AGCM (Atmospheric General Circulation Model) equipped with stable water isotope diagnostics.

CPD
10, 3421–3447, 2014

2 Methods

2.1 The classical estimation of past accumulation rates from water isotope data on the East Antarctic plateau

The physical link between the moisture content of air mass and its temperature has been systematically used to estimate past accumulation in Antarctica and establish ice core chronologies. This approach linking accumulation rate to temperature has been first proposed by Lorius et al. (1985) and Ritz (1992). Using a simple unidimensional model neglecting the possible changes in circulation intensity over the precipitation area, one infers that the precipitation rate at a time t equals its present-day value (at the time t_0) times the ratio of the derivatives vs. temperature T of the saturation vapour pressure over ice at times t and t_0:

$$A(t) = A(t_0) \times \frac{[\partial(P_{\text{sat}}/(T+273))/\partial T]_t}{[\partial(P_{\text{sat}}/(T+273))/\partial T]_{t_0}} \quad (1)$$

Where A is the accumulation rate and P_{sat} the saturation pressure over ice. The temperature considered in Eq. (1) is the temperature at condensation, approximated by the inversion temperature, T_{inv}, itself related to surface temperature T_s in Antarctica over a range from -15 to $-55\,^{\circ}$C (Jouzel and Merlivat, 1984) by:

$$T_{\text{inv}} = 0.67 \times T_s - 1.2 \quad (2)$$

where T_s is the mean near-surface atmospheric temperature either measured at 15 m deep in the firn or deduced from the average of the measured temperatures at 2 m height in weather station. This relation has been confirmed by Connolley (1996) and Ekaykin (2003) for the East Antarctic plateau.

In Antarctica, past temperature changes are classically retrieved from water isotope records in ice cores (δD or δ^{18}O) assuming that the present-day temperature/isotope

CPD
10, 3421–3447, 2014

spatial slope can be taken as a surrogate for the temporal slope at a given site. Using alternative methods to constrain past temperature in polar regions (combination of δ^{18}O and d-excess, (Vimeux et al., 2002), use of the isotopic composition of inert gases combined with firnification models, (Caillon et al., 2001), borehole temperature inversion, (Salamatin et al., 1998)), it has been shown that errors associated with this conventional approach are estimated to be of −10 to +30 % over glacial–interglacial transitions (Jouzel et al., 2003). However, a recent modelling experiment has suggested that error on the temperature reconstruction can reach up to 100 % for warmer interglacial periods (Sime et al., 2009).

The classical method for temperature reconstruction applied to sites in East Antarctica like Vostok, (Jouzel et al., 1987; Petit et al., 1999), Dome F (Watanabe et al., 2003) and EPICA Dome C (Jouzel et al., 2007), assumes that the temporal variations of δD, $\Delta\delta D$, are proportional to the temporal variations of surface temperature, ΔT_{surf}:

$$\Delta\delta D = 6.04 \times \Delta T_{\text{surf}} \tag{3}$$

Here the temperatures are expressed in °C.

The saturation vapor pressure over ice is linked with temperature and can be approximated in the range −70 °C to 0 °C by the following equation (Wagner and Pruß, 2002):

$$P_{\text{sat}}(T) = A \times 10^{\frac{mT}{T+T_n}} \tag{4}$$

with $A = 6.114742$, $m = 9.778707$ and $T_n = 273.1466$.

From the numerical solution of Eqs. (1) to (4) over the range of temperature variations observed in East Antarctica ice cores, it appears that the accumulation rate is exponentially linked to temperature. Keeping this idea of an exponential link, Parrenin et al. (2007a) and Bazin et al. (2013) have formulated the accumulation/isotope relation as:

$$A = A_0 \exp(\beta\Delta\delta D) \tag{5}$$

CPD
10, 3421–3447, 2014

Using ^{10}Be to test the validity of past accumulation rate reconstruction

A. Cauquoin et al.

where A_0 is an estimate of the present-day accumulation rate and β an adjustable parameter which is optimized during the chronology construction through chronological control points and an ice flow model (Parrenin et al., 2007b). While the accumulation rate reconstruction should be rather accurate for the upper part of the ice core, the uncertainties increase with depth because less chronological constraints are available and ice thinning becomes less predictable.

For the estimate of accumulation rate at Dome C with the EDC3 timescale, Parrenin et al. (2007a, b) have used an inverse method in order to get the best fit with a series of age markers (listed in Table 3 of Parrenin et al., 2007a). They have inferred the value of β in Eq. (5) as being equal to 0.0157, a value about 50 % higher than the one (0.0102) corresponding to the saturation vapour assumption (e.g. as derived from Eq. (1) and compared to the EDC3 accumulation rate on Fig. 2a).

More recently, during the construction of the AICC2012 chronology, the imposed relationship between δD and accumulation rate has been relaxed. The AICC2012 timescale (Bazin et al., 2013; Veres et al., 2013) has been developed for obtaining a coherent chronology between one Greenland ice core (NorthGRIP) and four Antarctic ice cores (EDC, EDML, TALDICE, Vostok) through the intensive use of relative tie points in the ice and gas phases of the different ice cores. In the chronological optimization process of AICC2012 performed by the DATICE Bayesian dating tool (Lemieux-Dudon et al., 2010), the scenario for both accumulation rate and thinning function for the different ice cores are allowed to vary freely, i.e. without an imposed relationship between accumulation rate and water isotopes as for the EDC3 chronology. Although the background scenario for EDC accumulation rate is the one given by Eq. (1), it is associated with a relatively large variance so that it is easily modified during the chronology optimization process. At the end, the amplitude of glacial–interglacial variations of accumulation rate over Termination 4 at Dome C is 5 % smaller in AICC2012 than in EDC3.

2.2 ^{10}Be measurements

The first procedure for measuring ^{10}Be in ice cores was described by Raisbeck et al. (1981b). Since then, efficiency has been greatly improved, both due to improvement of chemical procedures of the samples and AMS (Accelerator Mass Spectrometry) techniques (Raisbeck et al., 1987, 2007; Yiou et al., 1997). The ice from the Dome C ice core available for this study is a continuous series of "bag samples" (each measuring 55 cm) between 2384 and 2627 m deep. Each bag sample was cut into five pieces of 11 cm (weighting ~ 50 g) in order to obtain a high resolution ^{10}Be profile. This corresponds to around 2200 samples. The preparation of the samples was made at the Centre de Sciences Nucléaires et de Sciences de la Matière (CSNSM) in Orsay.

The current chemical procedure is described by Raisbeck et al. (2007). The samples were melted in a centrifuge cone, in the presence of 0.25 mg of ^{9}Be carrier. The $Be(OH)_2$ was then directly precipitated with ammonia (NH_4OH). The precipitate was extracted by centrifugation, then dissolved with 250 µL of nitric acid and 500 µL of highly pure water. The solution was transferred to a ceramic crucible to be dried on a hotplate and then heated to 900 °C during 45 min over an electric furnace in order to transform the precipitate to BeO. The beryllium oxyde was mixed with Niobium (Nb) powder and pressed into a copper cathode. The ^{10}Be/^{9}Be measurements were carried out at the ASTER (Accélérateur pour les Sciences de la Terre, Environnement, Risques) AMS facility at the Centre Européen de Recherche et d'Enseignement des Géosciences de l'Environnement (CEREGE) in Aix-en-Provence (Arnold et al., 2010), relative to the NIST (National Institute of Standards and Technology) Standard Reference Material (SRM) 4325, using the certified ratio of 2.68×10^{-11} ^{10}Be/^{9}Be. We are aware that many people now use the value of 2.79×10^{-11} given by Nishiizumi et al. (2007) for this standard. We have continued to use the value of 2.68 because it was in excellent agreement with the original home-made standard of the Orsay group (Raisbeck et al., 1978), and has been used for all our previous measurements. If desired, a conversion can be easily made, and will have no effect on relative values. The isobar

CPD
10, 3421–3447, 2014

^{10}B is suppressed by use of an absorber foil in the rare isotope path (Klein et al., 2008). The counting statistics lead to an uncertainty of typically 4 % for 1σ standard deviation. The chemical blanks produced with our ^{9}Be carrier used for the ice samples yielded an average process background $^{10}Be/^{9}Be$ of $(3.95 \pm 2.35) \times 10^{-15}$. In comparison, the $^{10}Be/^{9}Be$ ratios measured for EDC samples were on the order of 3.2×10^{-13}.

2.3 Models

In this study, we also want to test our experimental results by comparing them with the latest climate simulations of the last glacial maximum (LGM) and pre-industrial (PI) climates, obtained in the framework of the PMIP3 and CMIP5 projects (Braconnot et al., 2012). Both the PI and LGM climate simulations are equilibrium simulations, i.e. obtained by imposing non-evolving boundary conditions and forcings. Compared to the pre-industrial control simulation, LGM climate simulations are obtained by imposing the LGM ice sheet reconstructions (topography, albedo and land–sea mask differences due to sea-level lowering), the LGM atmospheric concentration of the main greenhouse gases as recorded by ice-cores and orbital forcing parameters for 21 000 years before present (following Berger, 1978). The experimental set-up is described in detail at the PMIP3 web site: http://pmip3.lsce.ipsl.fr/. The simulations used in this study are based on the CMIP5 database of October 2012.

In addition to the PMIP3 simulations we are using present-day and LGM simulation results obtained from the AGCM ECHAM5 (Roeckner et al., 2006) enhanced by stable water isotope diagnostics (Werner et al., 2011). For the LGM climate simulation, PMIP3-conform boundary conditions have been applied. Glacial sea surface temperatures and sea ice coverage has been derived from the GLAMAP Atlantic reconstruction data set (Schäfer-Neth and Paul, 2003). Both present-day and LGM simulation have been performed with a fine T106L31 spectral model resolution (horizontal grid box size of approx. 1.1° × 1.1°, 31 vertical levels).

CPD
10, 3421–3447, 2014

All used simulations are summarized in Table 1. From the different simulations we have used the following variables: T_{as} (near surface air temperature), *pr* (precipitation rate) and *sbl* (sublimation rate). As the sublimation rate was only available for 3 models out of 11 and as its values over the sites of interest were negligible compared to the precipitation rate in these models, we have not included the sublimation rate in the calculation of the accumulation rate changes from LGM to PI. We observe that T_{as} is systematically higher than the measured mean atmospheric temperature, which is a typical bias of AGCM in polar regions (see Risi et al., 2010). Then, the IPSL-CM5A-LR model gave us access to the modeled inversion temperatures. These data show that in the models, the slope of the relationship between T_{as} and the modeled inversion temperature is 15 % higher than the one given by Jouzel and Merlivat (1984) (cf. Eq. 2). However, when we use the modeled surface temperature T_{sm} (which is on average 4° lower than the simulated T_{as} values), we obtain a slope between T_{inv} and T_{sm} very close to the observed value of 0.67 (see Eq. 2). As a consequence and to artificially compensate for the cold bias of the AGCM, we have extracted both T_{as} and T_{sm} for the following calculations.

For ECHAM5, the values of the LGM–PI change in near-surface air temperature and precipitation rate are computed by performing a bilinear interpolation of the four nearest grid point values to the Dome C coordinates. For the other models, they are obtained by averaging the values of temperature and precipitation on a box of latitude [−77.6; −72.6] and longitude [120.85; 125.85].

3 From ^{10}Be concentrations to accumulation rate reconstruction

Figure 1a shows the high-resolution profile of ^{10}Be concentrations. The time resolution for the shown period varies between 20 years for MIS 9.3 and 70 years for MIS 10, the glacial period older than 340 kyr BP (Fig. 1f). We observe a strong anti-correlation between ^{10}Be concentration (Fig. 1a) and δD or δD-derived accumulation rate (Fig. 1b). This is not unexpected since ^{10}Be reaches the Antarctic plateau primarily by dry depo-

CPD
10, 3421–3447, 2014

sition so concentration of ^{10}Be in the ice is reduced for high accumulation periods. It has thus been proposed that ^{10}Be flux is a more appropriate parameter than concentration for estimating variations in ^{10}Be production (Yiou et al., 1985). This is illustrated in Fig. 1c showing the ^{10}Be flux as obtained by multiplying the ^{10}Be concentration times the accumulation rate from the EDC3 timescale (Parrenin et al., 2007a, b) and the density of ice.

Other potential contributions to ^{10}Be concentration variations are linked to (1) variations in the geomagnetic field intensity over centennial to millennial scales or (2) variations in the solar activity on secular timescales. For the influence of the geomagnetic field, we can make corrections by using independent estimates of the field intensity obtained by a stacked record of marine sediments (Channell et al., 2009). After synchronizing the time scale of the marine record with that of EDC (Cauquoin, 2013), we apply the theoretical estimate of Masarik and Beer (2009) on the relationship between ^{10}Be production and geomagnetic intensity, as shown in Fig. 1d. The main effect of this correction is to remove the long term decrease in the uncorrected ^{10}Be flux from 270 to 350 kyr BP. We have also looked at the theoretical estimate of Kovaltsov and Usoskin (2010) on the relationship between ^{10}Be production and geomagnetic field intensity, with very similar results.

Since we have no independent estimate of the solar variability during the time period being studied, we must assume that the average value of solar activity has been constant during this time. In reality, some of the remaining centennial structure in the ^{10}Be flux of Fig. 1e may be due to variations of solar activity, or to centennial geomagnetic variations not recorded by the marine cores. We now use the corrected ^{10}Be flux curve of Fig. 1e to estimate the ice accumulation rate of EDC during our time period. This procedure assumes that the spatial distribution of geomagnetically corrected ^{10}Be deposition remains constant with time, independent of climate.

In a first attempt to use ^{10}Be for such a reconstruction, we have chosen to keep the exponential link between accumulation and δD. Starting from the formulation proposed by Parrenin et al. (2007a), we have tried to adjust β in order to minimize the variance

CPD
10, 3421–3447, 2014

of the ^{10}Be flux signal while keeping consistency with the time scale of EDC3 (Fig. 2b). For this minimization, we have applied first a 100 year resampling to the ^{10}Be record. The variance is minimized for an increase of β by 5 % which corresponds to a larger glacial–interglacial amplitude by the same amount (the variance remains around its minimal value for β in the range 0.0160–0.0171). We also notice a general decrease of the variance by a factor 0.99 which supports this revision of accumulation rate estimate from δD over one glacial–interglacial cycle.

In a second attempt, we have performed a test with the assumption of a strictly constant ^{10}Be flux. The inferred accumulation is reported in Fig. 2c. The general shape of the accumulation rate reconstruction follows the evolution of the EDC3 accumulation rate. The main difference is a 16 % increase in the accumulation over the optimum of MIS 9.3. Even if the assumption of a strictly constant ^{10}Be flux is not realistic, we have tested if the inferred accumulation rate is consistent with chronological constraints (Table 2). For this aim, we have imposed this accumulation rate as a background accumulation rate scenario for EDC in the DATICE tool for chronology optimization with a very small associated variance. The other background scenarios for the 4 other ice cores (NorthGRIP, EDML, Taldice, Vostok) are kept identical as those of AICC2012 (Bazin et al., 2013; Veres et al., 2013). With such background accumulation rate for EDC, the minimization of DATICE is easily reached with very small modifications of the thinning function, well within the imposed variance, compared to the AICC2012 chronology.

The existence of a strong link between past changes in accumulation and temperature is confirmed to first order by our ^{10}Be approach and we next examine how paleoclimate simulations performed with different GCMs might reveal further insight on this link between accumulation and temperature.

4 Accumulation vs. temperature/δD relationship in East Antarctica

The relationship between accumulation rate and temperature in East Antarctica is a consequence of simple thermodynamic laws linking the maximum moisture con-

CPD
10, 3421–3447, 2014

tent and the mean temperature of the air. These physical laws are implemented in Atmospheric General Circulation Models (AGCM). The models should thus properly predict the physical links between accumulation rate and temperature in East Antarctica. Therefore we compare AGCM outputs, from the models described in Sect. 2.3, with the accumulation rate reconstruction presented in the previous section.

Figure 3a shows a compilation of accumulation rate and temperature change for the 11 different AGCMs included in the PMIP3/CMIP5 coupled models and for the ECHAM5 simulation, between the LGM and the present-day. We have chosen to focus only on the relationship between the change in accumulation rate and the change in temperature between the LGM and present-day. Indeed, we can hardly discuss absolute levels of temperature and accumulation rate for two reasons. First, the AGCM models are known to overestimate temperature on the East Antarctic plateau. Second, our ^{10}Be data are not covering the last deglaciation as the model simulations but the transition occurring between MIS 10 and MIS 9 which has larger associated temperature and accumulation rate increases than the last deglaciation (Fig. 3a). Still the accumulation rate vs. temperature slope reconstructed from water isotopes in ice core is the same for the transition between MIS 10 and MIS 9 and the last deglaciation. We have also checked that the model results shown on Fig. 3a do not change if we replace the ΔT_s calculation based on the near-surface air temperature (T_{as}) by one based on surface temperature (T_{sm}). Finally, we have tested with the IPSL-CM5A-LR model the influence of the topography changes on the temperature vs. accumulation rate slope by keeping an identical Antarctic ice cap for the LGM and present-day conditions and verifying that the relationship remains the same.

Despite the different amplitudes of temperature and accumulation rate changes between data and model over a glacial–interglacial transition, we observe a general agreement in the accumulation rate vs. temperature slope (Fig. 3a). Both model and data suggest an average slope of 0.23 cm ie yr^{-1} °C^{-1}. Still, the difference in the accumulation rate vs. temperature relationship between different GCM simulations is much larger (100 %) than for our different reconstructions based on ^{10}Be flux and/or chrono-

CPD
10, 3421–3447, 2014

logical constraints (16 %). The slope based on the relationship between accumulation rate and saturation pressure over ice is 28 % lower (brown line on Fig. 3a). Note that we did not take into account here the uncertainty in the amplitude of the temperature reconstruction from the measured water isotopes data. However, it is estimated to be relatively small and of the same order than our uncertainties in accumulation rate reconstruction (within −10 to +30 % for glacial–interglacial variations in East Antarctica, Jouzel et al., 2003).

Finally, to avoid any assumption on the relationship between water isotopes and temperature, we have directly compared the accumulation rate on water isotopes variations for both ice core data and AGCM model results (Fig. 3b). In our study, only one model (ECHAM5) is equipped with water isotopes diagnostics. As it was also observed for the temperature change, the δD increase during the deglaciation is smaller in the ECHAM5 simulations than in ice core records. However the slope of accumulation rate vs. δD given by ECHAM5 compares very well with our different accumulation rate vs. δD slope inferred from both water isotopes and ^{10}Be. Only the slope deduced from the saturation vapor pressure formulation is lower by ~ 30 %. The accumulation rate vs. temperature changes slope of ECHAM5 is smaller than the one reconstructed from water isotopes in ice core. This could mean that the δD–temperature slope is underevaluated in the model compared to the hypothesis of the spatial relationship between precipitation isotopic composition and local temperature (Lorius et al., 1969). But given the uncertainties and the lack of models equipped with water isotope diagnostics, it is difficult to conclude on this point.

5 Conclusions

We have produced the first record of ^{10}Be concentration at high resolution in an ice core over a whole climatic cycle (355 to 269 kyr BP). After correction for geomagnetic intensity, the variations in ^{10}Be concentration are believed to be mainly linked to variations in the accumulation rate of snow. We have used this property to test the validity

CPD
10, 3421–3447, 2014

of the classical accumulation rate reconstruction method on the EDC ice core. We have shown that the classical estimation of accumulation rate variations from records of water isotopes is in agreement with the ^{10}Be based estimate within a possible underestimation of 16 %. This uncertainty of the accumulation rate reconstruction from water isotopes is of the same order of magnitude than the uncertainty of the temperature reconstruction from water isotopes in Antarctic ice cores (−10 to +30 %, Jouzel et al., 2003). This result strengthens the quantitative results that can be obtained using water isotopic records in ice cores from the East Antarctic plateau in terms of accumulation rate and temperature reconstruction. Finally, the relationship between temperature and accumulation rate is comparable when using water isotopic inferred data and results from several AGCM simulations for LGM–PI climate changes despite a larger spread in the model outputs. This agreement indicates that the thermodynamic law linking moisture content in the air and temperature implemented in the GCMs leads to realistic results even in polar regions, at the end of the water distillation trajectory.

Acknowledgements. This work is a contribution to the European Project for Ice Coring in Antarctica (EPICA), a joint European Science Foundation/European Commission (EC) scientific programme, funded by the EC and by national contributions from Belgium, Denmark, France, Germany, Italy, the Netherlands, Norway, Sweden, Switzerland and the UK. The main logistic support was provided by IPEV and PNRA. We acknowledge the World Climate Research Programme's Working Group on Coupled Modelling, which is responsible for CMIP and the Paleoclimate Modelling Intercomparison Project (PMIP). We thank the climate modeling groups (listed in Table 1 of this paper) for producing and making available their model output. For CMIP the US Department of Energy's Program for Climate Model Diagnosis and Intercomparison provides coordinating support and led development of software infrastructure in partnership with the Global Organization for Earth System Science Portals. This work was funded by the French ANR project Dome A and the ERC Grant COMBINISO project no. 306045. The ASTER AMS national facility (CEREGE, Aix en Provence) is supported by the INSU/CNRS, the ANR through the "Projets thématiques d'excellence" program for the "Equipements d'Excellence" ASTER-CEREGE action, IRD, and CEA.

References

Arnold, M., Merchel, S., Bourlès, D. L., Braucher, R., Benedetti, L., Finkel, R. C., Aumaître, G., Gottdang, A., and Klein, M.: The French accelerator mass spectrometry facility ASTER: improved performance and developments, Nucl. Instrum. Meth. B, 268, 1954–1959, doi:10.1016/j.nimb.2010.02.107, 2010. 3429

Bazin, L., Landais, A., Lemieux-Dudon, B., Toyé Mahamadou Kele, H., Veres, D., Parrenin, F., Martinerie, P., Ritz, C., Capron, E., Lipenkov, V., Loutre, M.-F., Raynaud, D., Vinther, B., Svensson, A., Rasmussen, S. O., Severi, M., Blunier, T., Leuenberger, M., Fischer, H., Masson-Delmotte, V., Chappellaz, J., and Wolff, E.: An optimized multi-proxy, multi-site Antarctic ice and gas orbital chronology (AICC2012): 120–800 ka, Clim. Past, 9, 1715–1731, doi:10.5194/cp-9-1715-2013, 2013. 3427, 3428, 3433, 3444

Berger, A. L.: Long-term variations of daily insolation and quaternary climatic changes, J. Atmos. Sci., 35, 2362–2367, doi:10.1175/1520-0469(1978)035<2362:LTVODI>2.0.CO;2, 1978. 3430

Blunier, T., Spahni, R., Barnola, J.-M., Chappellaz, J., Loulergue, L., and Schwander, J.: Synchronization of ice core records via atmospheric gases, Clim. Past, 3, 325–330, doi:10.5194/cp-3-325-2007, 2007. 3424

Braconnot, P., Harrison, S. P., Kageyama, M., Bartlein, P. J., Masson-Delmotte, V., Abe-Ouchi, A., Otto-Bliesner, B., and Zhao, Y.: Evaluation of climate models using palaeoclimatic data, Nature Climate Change, 2, 417–424, doi:10.1038/nclimate1456, 2012. 3430

Caillon, N., Severinghaus, J. P., Barnola, J.-M., Chappellaz, J., Jouzel, J., and Parrenin, F.: Estimation of temperature change and of gas age-ice age difference, 108 kyr B. P., at Vostok, Antarctica, J. Geophys. Res., 106, 31893, doi:10.1029/2001JD900145, 2001. 3427

Cauquoin, A.: Flux de ^{10}Be en Antarctique durant les 800 000 dernières années et interprétation, Ph.D. thesis, Université Paris-Sud 11, 2013. 3432

Channell, J. E. T., Xuan, C., and Hodell, D. A.: Stacking paleointensity and oxygen isotope data for the last 1.5 Myr (PISO-1500), Earth Planet. Sc. Lett., 283, 14–23, doi:10.1016/j.epsl.2009.03.012, 2009. 3432, 3445

Connolley, W. M.: The Antarctic temperature inversion, Int. J. Climatol., 16, 1333–1342, doi:10.1002/(SICI)1097-0088(199612)16:12<1333::AID-JOC96>3.3.CO;2-Y, 1996. 3426

Ekaykin, A.: Meteorological regime of central Antarctica and its role in the formation of isotope composition of snow thickness, Ph.D. thesis, Université Joseph Fourier – Grenoble I, 2003. 3426

EPICA Community Members: Eight glacial cycles from an Antarctic ice core, Nature, 429, 623–628, doi:10.1038/nature02599, 2004. 3424

Guillevic, M., Bazin, L., Landais, A., Kindler, P., Orsi, A., Masson-Delmotte, V., Blunier, T., Buchardt, S. L., Capron, E., Leuenberger, M., Martinerie, P., Prié, F., and Vinther, B. M.: Spatial gradients of temperature, accumulation and δ^{18}O-ice in Greenland over a series of Dansgaard–Oeschger events, Clim. Past, 9, 1029–1051, doi:10.5194/cp-9-1029-2013, 2013. 3424

Jouzel, J. and Merlivat, L.: Deuterium and oxygen 18 in precipitation: modeling of the isotopic effects during snow formation, J. Geophys. Res., 89, 11749, doi:10.1029/JD089iD07p11749, 1984. 3426, 3431

Jouzel, J., Genthon, C., Lorius, C., Petit, J. R., and Barkov, N. I.: Vostok ice core – a continuous isotope temperature record over the last climatic cycle (160,000 years), Nature, 329, 403–408, doi:10.1038/329403a0, 1987. 3427

Jouzel, J., Raisbeck, G., Benoist, J. P., Yiou, F., Lorius, C., Raynaud, D., Petit, J. R., Barkov, N. I., Korotkevitch, Y. S., and Kotlyakov, V. M.: A comparison of deep Antarctic ice cores and their implications for climate between 65,000 and 15,000 years ago, Quaternary Res., 31, 135–150, doi:10.1016/0033-5894(89)90003-3, 1989. 3425

Jouzel, J., Vimeux, F., Caillon, N., Delaygue, G., Hoffmann, G., Masson-Delmotte, V., and Parrenin, F.: Magnitude of isotope/temperature scaling for interpretation of central Antarctic ice cores, J. Geophys. Res., 108, 4361, doi:10.1029/2002JD002677, 2003. 3427, 3435, 3436

Jouzel, J., Masson-Delmotte, V., Cattani, O., Dreyfus, G., Falourd, S., Hoffmann, G., Minster, B., Nouet, J., Barnola, J.-M., Blunier, T., Chappellaz, J., Fischer, H., Gallet, J. C., Johnsen, S., Leuenberger, M., Loulergue, L., Luethi, D., Oerter, H., Parrenin, F., Raisbeck, G., Raynaud, D., Schilt, A., Schwander, J., Delmo, E., Souchez, R., Spahni, R., Stauffer, B., Steffensen, J. P., Stenni, B., Stocker, T. F., Tison, J. L., Werner, M., and Wolff, E.: Orbital and millennial Antarctic climate variability over the past 800,000 years, Science, 317, 793–796, doi:10.1126/science.1141038, 2007. 3427, 3445

Klein, M. G., Gottdang, A., Mous, D. J. W., Bourlès, D. L., Arnold, M., Hamelin, B., Aumaitre, G., Braucher, R., Merchel, S., and Chauvet, F.: Performance of the HVE 5 MV AMS system at

CEREGE using an absorber foil for isobar suppression, Nucl. Instrum. Meth. B, 266, 1828–1832, doi:10.1016/j.nimb.2007.11.077, 2008. 3430

Kovaltsov, G. A. and Usoskin, I. G.: A new 3D numerical model of cosmogenic nuclide ^{10}Be production in the atmosphere, Earth Planet. Sc. Lett., 291, 182–188, doi:10.1016/j.epsl.2010.01.011, 2010. 3432

Lal, D. and Peters, B.: Cosmic ray produced radioactivity on the Earth, in: Kosmische Strahlung II/Cosmic Rays II, edited by: Sittle, K., vol. 46/2 of Handbuch der Physik, Springer-Verlag, Berlin, doi:10.1007/978-3-642-46079-1_7, 551–612, 1967. 3424

Langereis, C. G., Dekkers, M. J., Lange, G. J., Paterne, M., and Santvoort, P. J. M.: Magnetostratigraphy and astronomical calibration of the last 1.1 Myr from an eastern Mediterranean piston core and dating of short events in the Brunhes, Geophys. J. Int., 129, 75–94, doi:10.1111/j.1365-246X.1997.tb00938.x, 1997. 3425

Lemieux-Dudon, B., Blayo, E., Petit, J.-R., Waelbroeck, C., Svensson, A., Ritz, C., Barnola, J.-M., Narcisi, B. M., and Parrenin, F.: Consistent dating for Antarctic and Greenland ice cores, Quaternary Sci. Rev., 29, 8–20, doi:10.1016/j.quascirev.2009.11.010, 2010. 3428

Lipenkov, V. Y., Raynaud, D., Loutre, M. F., and Duval, P.: On the potential of coupling air content and O_2/N_2 from trapped air for establishing an ice core chronology tuned on local insolation, Quaternary Sci. Rev., 30, 3280–3289, doi:10.1016/j.quascirev.2011.07.013, 2011. 3444

Lorius, C., Merlivat, L., and Hagemann, R.: Variation in the mean deuterium content of precipitations in Antarctica, J. Geophys. Res., 74, 7027–7031, doi:10.1029/JC074i028p07027, 1969. 3435

Lorius, C., Ritz, C., Jouzel, J., Merlivat, L., and Barkov, N. I.: A 150,000-year climatic record from Antarctic ice, Nature, 316, 591–596, doi:10.1038/316591a0, 1985. 3426

Masarik, J. and Beer, J.: An updated simulation of particle fluxes and cosmogenic nuclide production in the Earth's atmosphere, J. Geophys. Res., 114, D11103, doi:10.1029/2008JD010557, 2009. 3432, 3445

NEEM Community Members: Eemian interglacial reconstructed from a Greenland folded ice core, Nature, 493, 489–494, doi:10.1038/nature11789, 2013. 3424

Nishiizumi, K., Imamura, M., Caffee, M. W., Southon, J. R., Finkel, R. C., and McAninch, J.: Absolute calibration of ^{10}Be AMS standards, Nucl. Instrum. Meth. B, 258, 403–413, doi:10.1016/j.nimb.2007.01.297, 2007. 3429

North Greenland Ice Core Project Members: High-resolution record of Northern Hemisphere climate extending into the last interglacial period, Nature, 431, 147–151, doi:10.1038/nature02805, 2004. 3423

Parrenin, F., Dreyfus, G., Durand, G., Fujita, S., Gagliardini, O., Gillet, F., Jouzel, J., Kawamura, K., Lhomme, N., Masson-Delmotte, V., Ritz, C., Schwander, J., Shoji, H., Uemura, R., Watanabe, O., and Yoshida, N.: 1-D-ice flow modelling at EPICA Dome C and Dome Fuji, East Antarctica, Clim. Past, 3, 243–259, doi:10.5194/cp-3-243-2007, 2007a. 3427, 3428, 3432, 3446

Parrenin, F., Barnola, J.-M., Beer, J., Blunier, T., Castellano, E., Chappellaz, J., Dreyfus, G., Fischer, H., Fujita, S., Jouzel, J., Kawamura, K., Lemieux-Dudon, B., Loulergue, L., Masson-Delmotte, V., Narcisi, B., Petit, J.-R., Raisbeck, G., Raynaud, D., Ruth, U., Schwander, J., Severi, M., Spahni, R., Steffensen, J. P., Svensson, A., Udisti, R., Waelbroeck, C., and Wolff, E.: The EDC3 chronology for the EPICA Dome C ice core, Clim. Past, 3, 485–497, doi:10.5194/cp-3-485-2007, 2007b. 3428, 3432, 3445, 3446

Petit, J. R., Jouzel, J., Raynaud, D., Barkov, N. I., Barnola, J.-M., Basile, I., Bender, M., Chappellaz, J., Davis, M., Delaygue, G., Delmotte, M., Kotlyakov, V. M., Legrand, M., Lipenkov, V. Y., Lorius, C., Pépin, L., Ritz, C., Saltzman, E., and Stievenard, M.: Climate and atmospheric history of the past 420,000 years from the Vostok ice core, Antarctica, Nature, 399, 429–436, doi:10.1038/20859, 1999. 3427

Raisbeck, G. M., Yiou, F., Fruneau, M., and Loiseaux, J. M.: Beryllium-10 mass spectrometry with a cyclotron, Science, 202, 215–217, doi:10.1126/science.202.4364.215, 1978. 3429

Raisbeck, G. M., Yiou, F., Fruneau, M., Loiseaux, J. M., Lieuvin, M., and Ravel, J. C.: Cosmogenic $^{10}Be/^{7}Be$ as a probe of atmospheric transport processes, Geophys. Res. Lett., 8, 1015–1018, doi:10.1029/GL008i009p01015, 1981a. 3424

Raisbeck, G. M., Yiou, F., Fruneau, M., Loiseaux, J. M., Lieuvin, M., Ravel, J. C., and Lorius, C.: Cosmogenic ^{10}Be concentrations in Antarctic ice during the past 30,000 years, Nature, 292, 825, doi:10.1038/292825a0, 1981b. 3429

Raisbeck, G. M., Yiou, F., Bourlès, D., Lorius, C., and Jouzel, J.: Evidence for two intervals of enhanced ^{10}Be deposition in Antarctic ice during the last glacial period, Nature, 326, 273–277, doi:10.1038/326273a0, 1987. 3429

Raisbeck, G. M., Yiou, F., Jouzel, J., and Stocker, T. F.: Direct north-south synchronization of abrupt climate change record in ice cores using Beryllium 10, Clim. Past, 3, 541–547, doi:10.5194/cp-3-541-2007, 2007. 3429

CPD
10, 3421–3447, 2014

Using ^{10}Be to test the validity of past accumulation rate reconstruction

A. Cauquoin et al.

Raynaud, D., Lipenkov, V., Lemieux-Dudon, B., Duval, P., Loutre, M.-F., and Lhomme, N.: The local insolation signature of air content in Antarctic ice. A new step toward an absolute dating of ice records, Earth Planet. Sc. Lett., 261, 337–349, doi:10.1016/j.epsl.2007.06.025, 2007. 3444

Risi, C., Bony, S., Vimeux, F., and Jouzel, J.: Water-stable isotopes in the LMDZ4 general circulation model: model evaluation for present-day and past climates and applications to climatic interpretations of tropical isotopic records, J. Geophys. Res., 115, D12118, doi:10.1029/2009JD013255, 2010. 3431

Ritz, C.: Un modèle thermo-mécanique d'évolution pour le bassin glaciaire Antarctique Vostok-Glacier Byrd: Sensibilité aux valeurs des paramètres mal connus, Ph.D. thesis, Université Joseph Fourier – Grenoble I, 1992. 3426

Roeckner, E., Brokopf, R., Esch, M., Giorgetta, M., Hagemann, S., Kornblueh, L., Manzini, E., Schlese, U., and Schulzweida, U.: Sensitivity of simulated climate to horizontal and vertical resolution in the ECHAM5 atmosphere model, J. Climate, 19, 3771, doi:10.1175/JCLI3824.1, 2006. 3430

Salamatin, A. N., Lipenkov, V. Y., Barkov, N. I., Jouzel, J., Petit, J. R., and Raynaud, D.: Ice core age dating and paleothermometer calibration based on isotope and temperature profiles from deep boreholes at Vostok Station (East Antarctica), J. Geophys. Res., 103, 8963–8977, doi:10.1029/97JD02253, 1998. 3427

Schäfer-Neth, C. and Paul, A.: Gridded Global LGM SST and Salinity Reconstruction, IGBP PAGES/World Data Center for Paleoclimatology, Boulder. Data Contribution Series #2003-046., NOAA/NGDC Paleoclimatology Program, Boulder CO, USA, available at: ftp://ftp.ncdc.noaa.gov/pub/data/paleo/contributions_by_author/paul2003, 2003. 3430

Sime, L. C., Wolff, E. W., Oliver, K. I. C., and Tindall, J. C.: Evidence for warmer interglacials in East Antarctic ice cores, Nature, 462, 342–345, doi:10.1038/nature08564, 2009. 3427

Singer, B. S., Guillou, H., Jicha, B. R., Laj, C., Kissel, C., Beard, B. L., and Johnson, C. M.: $^{40}Ar/^{39}Ar$, K-Ar and $^{230}Th – ^{238}U$ dating of the Laschamp excursion: a radioisotopic tie-point for ice core and climate chronology, Earth Planet. Sc. Lett., 286, 80–88, doi:10.1016/j.epsl.2009.06.030, 2009. 3425

Suwa, M. and Bender, M. L.: Chronology of the Vostok ice core constrained by O_2/N_2 ratios of occluded air, and its implication for the Vostok climate records, Quaternary Sci. Rev., 27, 1093–1106, doi:10.1016/j.quascirev.2008.02.017, 2008. 3444

Taylor, K. E., Balaji, V., Hankin, S., Juckes, M., Lawrence, B., and Pascoe, S.: CMIP5 Data Reference Syntax (DRS) and Controlled Vocabularies, version 1.3.1, available at: http://cmip-pcmdi.llnl.gov/cmip5/docs/cmip5_data_reference_syntax.pdf, 2012. 3443

Thouveny, N., Bourlès, D. L., Saracco, G., Carcaillet, J. T., and Bassinot, F.: Paleoclimatic context of geomagnetic dipole lows and excursions in the Brunhes, clue for an orbital influence on the geodynamo?, Earth Planet. Sc. Lett., 275, 269–284, doi:10.1016/j.epsl.2008.08.020, 2008. 3425

van Ommen, T. D. and Morgan, V.: Calibrating the ice core paleothermometer using seasonality, J. Geophys. Res., 102, 9351–9358, doi:10.1029/96JD04014, 1997. 3424

Veres, D., Bazin, L., Landais, A., Toyé Mahamadou Kele, H., Lemieux-Dudon, B., Parrenin, F., Martinerie, P., Blayo, E., Blunier, T., Capron, E., Chappellaz, J., Rasmussen, S. O., Severi, M., Svensson, A., Vinther, B., and Wolff, E. W.: The Antarctic ice core chronology (AICC2012): an optimized multi-parameter and multi-site dating approach for the last 120 thousand years, Clim. Past, 9, 1733–1748, doi:10.5194/cp-9-1733-2013, 2013. 3428, 3433

Vimeux, F., Cuffey, K. M., and Jouzel, J.: New insights into Southern Hemisphere temperature changes from Vostok ice cores using deuterium excess correction, Earth Planet. Sc. Lett., 203, 829–843, doi:10.1016/S0012-821X(02)00950-0, 2002. 3427

Wagner, W. and Pruß, A.: The IAPWS formulation 1995 for the thermodynamic properties of ordinary water substance for general and scientific use, J. Phys. Chem. Ref. Data, 31, 387, doi:10.1063/1.1461829, 2002. 3427

Watanabe, O., Jouzel, J., Johnsen, S., Parrenin, F., Shoji, H., and Yoshida, N.: Homogeneous climate variability across East Antarctica over the past three glacial cycles, Nature, 422, 509–512, doi:10.1038/nature01525, 2003. 3427

Werner, M., Langebroek, P. M., Carlsen, T., Herold, M., and Lohmann, G.: Stable water isotopes in the ECHAM5 general circulation model: Toward high-resolution isotope modeling on a global scale, J. Geophys. Res., 116, D15109, doi:10.1029/2011JD015681, 2011. 3430

Yiou, F., Raisbeck, G. M., Bourles, D., Lorius, C., and Barkov, N. I.: ^{10}Be in ice at Vostok Antarctica during the last climatic cycle, Nature, 316, 616–617, doi:10.1038/316616a0, 1985. 3425, 3432

Yiou, F., Raisbeck, G. M., Baumgartner, S., Beer, J., Hammer, C., Johnsen, S., Jouzel, J., Kubik, P. W., Lestringuez, J., Stiévenard, M., Suter, M., and Yiou, P.: Beryllium 10 in the Greenland Ice Core Project ice core at Summit, Greenland, J. Geophys. Res., 102, 26783–26794, doi:10.1029/97JC01265, 1997. 3429

Table 1. List of all simulations used in this study (see Fig. 3). The ensemble member (r⟨*N*⟩i⟨*M*⟩p⟨*L*⟩) formatted as shown below (e.g. "r3i1p21" with r for "realization", i for "initialization method indicator" and p for "perturbed physics") distinguishes among closely related simulations by a single model (Taylor et al., 2012).

Institute	Model	Model institution	CMIP5 experiment Model *ensemble member* used (r⟨*N*⟩i⟨*M*⟩p⟨*L*⟩) 0k piControl	 21k lgm
CNRM-CERFACS	CNRM-CM5	Centre National de Recherches Météorologiques/Centre Européen de Recherche et Formation Avancée en Calcul Scientifique, France	r1i1p1 (CNRM-CM5)	r1i1p1 (CNRM-CM5)
NASA-GISS	GISS-E2-R	NASA Goddard Institute for Space Studies, US	r1i1p142 (GISS-E2-R_p150) r1i1p142 (GISS-E2-R_p151)	r1i1p150 (GISS-E2-R_p150) r1i1p151 (GISS-E2-R_p151)
IPSL	IPSL-CM5A-LR	Institut Pierre-Simon Laplace, France	r1i1p1 (IPSL-CM5A-LR)	r1i1p1 (IPSL-CM5A-LR)
LASC-CESS	FGOALS-g2	LASG, Institute of Atmospheric Physics, Chinese Academy of Sciences and CESS, Tsinghua University, China	r1i1p1 (FGOALS-g2)	r1i1p1 (FGOALS-g2)
MIROC	MIROC-ESM	Japan Agency for Marine-Earth Science and Technology, Atmosphere and Ocean Research Institute (The University of Tokyo), and National Institute for Environmental Studies, Japan	r1i1p1 (MIROC-ESM)	r1i1p1 (MIROC-ESM)
MPI-M	MPI-ESM-P ECHAM5	Max Planck Institute for Meteorology, Hamburg, Germany	r1i1p1 (MPI-ESM-P_p1) r1i1p1 (MPI-ESM-P_p2) ECHAM5	r1i1p1 (MPI-ESM-P_p1) r1i1p2 (MPI-ESM-P_p1) ECHAM5
MRI	MRI-CGCM3	Meteorological Research Institute, Tsukuba, Japan	r1i1p1 (MRI-CGCM3)	r1i1p1 (MRI-CGCM3)
NCAR	CCSM4	National Center for Atmospheric Research, US/Dept. of Energy/NSF	r1i1p1 (CCSM4_r1) r2i1p1 (CCSM4_r2)	r1i1p1 (CCSM4_r1) r2i1p1 (CCSM4_2)

CPD
10, 3421–3447, 2014

Using ^{10}Be to test the validity of past accumulation rate reconstruction

A. Cauquoin et al.

Table 2. List of markers used to constrain EDC and Vostok ice cores between 269 and 355 kyr BP for the AICC2012 chronology. References ("Ref."): (1) Suwa and Bender (2008) (2) Lipenkov et al. (2011) (3) Raynaud et al. (2007) (4) Bazin et al. (2013).

Vostok age markers	Depth	Age	Uncertainty	Type of markers	Ref.
Ice age markers	2882.1	275 200	4000	$\delta O_2/N_2$	1
	2883.02	275 950	6343	air content	2
	2912.1	286 300	4000	$\delta O_2/N_2$	1
	2962.7	296 800	4000	$\delta O_2/N_2$	1
	3005.6	307 700	4000	$\delta O_2/N_2$	1
	3011	307 950	6424	air content	2
	3040.7	319 200	4000	$\delta O_2/N_2$	1
	3043.04	318 950	6308	air content	2
	3080.5	330 000	4000	$\delta O_2/N_2$	1
	3130.6	339 700	4000	$\delta O_2/N_2$	1
	3145.95	346 950	6527	air content	2
	3157.1	349 200	4000	$\delta O_2/N_2$	1
Gas age markers	2887	272 900	6000	$\delta^{18}O_{atm}$	1
	2947.6	285 900	6000	$\delta^{18}O_{atm}$	1
	2990.3	297 500	6000	$\delta^{18}O_{atm}$	1
	3026.9	308 300	6000	$\delta^{18}O_{atm}$	1
	3062.5	318 300	6000	$\delta^{18}O_{atm}$	1
	3101.4	329 000	6000	$\delta^{18}O_{atm}$	1
	3146.2	340 300	6000	$\delta^{18}O_{atm}$	1
	3173.8	351 000	6000	$\delta^{18}O_{atm}$	1
EDC age markers					
Ice age markers	2500.25	306 950	6652	air content	3
	2510.75	318 950	6242	air content	3
	2610.8	346 950	7120	air content	3
Stratigraphic links between EDC and Vostok					
	Depth EDC	Depth Vostok	Uncertainty	Type of markers	Ref.
	2419.34	2911.06	1500	CH_4	4
	2451.33	2954.61	1500	CH_4	4
	2501.4	3018.01	1500	CH_4	4
	2521.2	3051.5	1500	CH_4	4
	2544.83	3079.41	1500	CH_4	4
	2583.9	3123.5	1500	CH_4	4
	2613	3162.8	1500	CH_4	4

CPD
10, 3421–3447, 2014

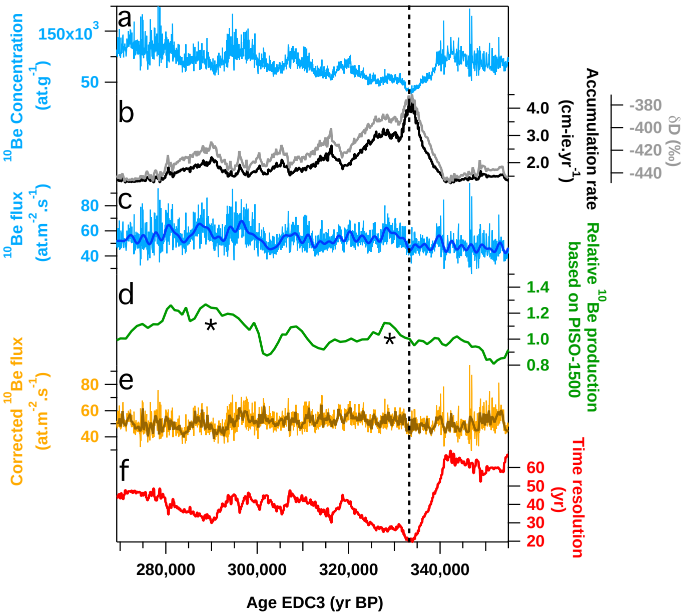

Figure 1. High resolution ^{10}Be data between 2384 and 2627 m deep (269–355 kyr BP on EDC3 age scale). **(a)** Raw ^{10}Be concentrations (at g^{-1}). **(b)** In grey, δD profile at EDC including the interglacial period MIS 9.3 (Jouzel et al., 2007). In black, the accumulation rate of the site (cm ie yr^{-1}) (Parrenin et al., 2007b). **(c)** Calculated ^{10}Be flux using EDC3 accumulation rate. The light-blue curve corresponds to raw data, the bold-blue curve is the low-pass filtered ^{10}Be flux (1/2000 yr^{-1}). The dotted line corresponds to a local minimum in ^{10}Be flux, coincident with the maximum of accumulation. **(d)** ^{10}Be production based on paleointensity record PISO-1500 (Channell et al., 2009) on EDC3 age scale and calculated using calculations of Masarik and Beer (2009). The asterisks show the possible correlation with proposed geomagnetic events, Portuguese Margin (~ 290 kyr BP) and Calabrian Ridge 1 (~ 320 kyr BP). **(e)** Raw and 100 yr resampled ^{10}Be flux corrected by PISO-1500. **(f)** Time resolution of the ^{10}Be profile (difference between the n and $n+1$ sample ages).

CPD
10, 3421–3447, 2014

Using ^{10}Be to test the validity of past accumulation rate reconstruction

A. Cauquoin et al.

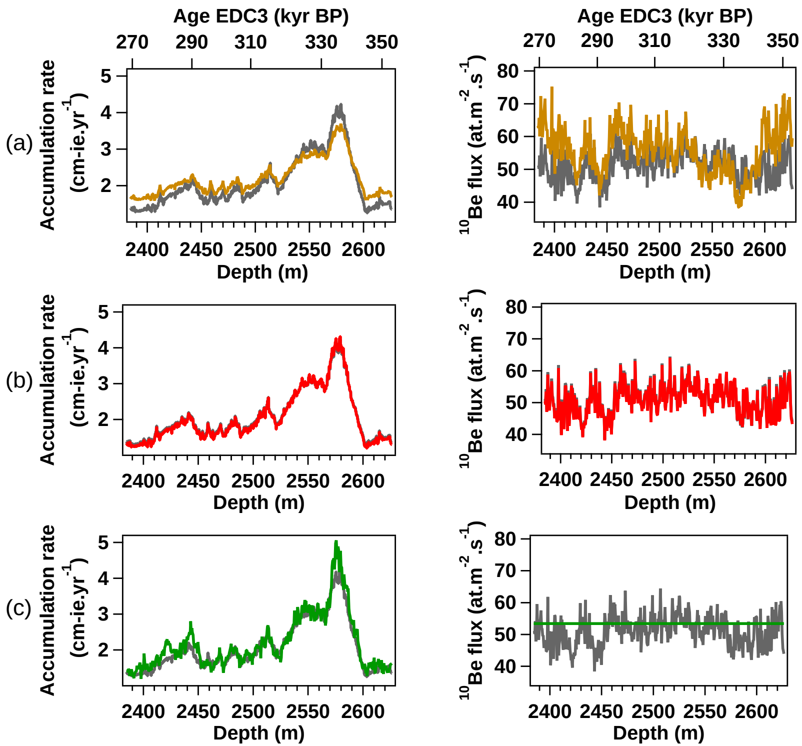

Figure 2. Several accumulation rate reconstructions (left column) and the corresponding ^{10}Be flux corrected by PISO-1500 (right column) discussed in Sect. 3. The initial reconstruction (EDC3 from Parrenin et al., 2007a, b) is shown in grey. **(a)** Saturation vapor pressure formulation **(b)** Optimization of the interglacial–glacial amplitude coefficient (β) by minimization of the variance of the ^{10}Be flux corrected for past variations of geomagnetic field intensity (red curves) **(c)** Accumulation rate assuming a constant ^{10}Be flux (fixed at 53.44 at m^{-2} s^{-1} over the whole period).

CPD
10, 3421–3447, 2014

Using ^{10}Be to test the validity of past accumulation rate reconstruction

A. Cauquoin et al.

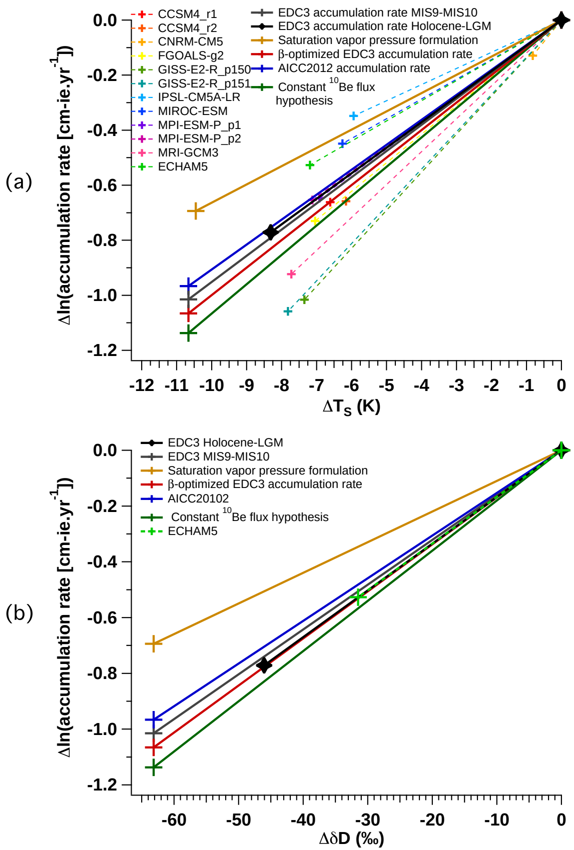

Figure 3. (a) Accumulation rate vs. temperature change for 12 different GCMs between the LGM and the present-day and comparison with the relationships from EDC3 (last deglaciation and MIS 9.3) and our reconstructions (average during the glacial and the interglacial period). **(b)** Accumulation rate vs. δD change for both ice core data and ECHAM5 simulation results.

CPD
10, 3421–3447, 2014